ISSN 0036-0236, Russian Journal of Inorganic Chemistry, 2022, Vol. 67, No. 6, pp. 754–760. © Pleiades Publishing, Ltd., 2022.
Russian Text © The Author(s), 2022, published in Zhurnal Neorganicheskoi Khimii, 2022, Vol. 67, No. 6, pp. 678–685.

SYNTHESIS AND PROPERTIES OF INORGANIC COMPOUNDS

High-Temperature Properties of Layered Oxides $(La,Tb,Sr)_2CuO_{4\pm\delta}$ with T*-Structure

S. Ya. Istomin[a], *, A. V. Morozov[a], N. V. Lyskov[b], S. M. Kazakov[a], and E. V. Antipov[a]

[a] *Faculty of Chemistry, Moscow State University, Moscow 119991 Russia*

[b] *Institute of Problems of Chemical Physics, Russian Academy of Sciences, Chernogolovka, Moscow oblast, 142432 Russia*

**e-mail: isserge71@gmail.com*

Received October 12, 2021; revised November 8, 2021; accepted November 15, 2021

Abstract—The high-temperature thermal expansion and electrical conductivity of the T*-phase cuprates $La_{1.2-x}Sr_xTb_{0.8}CuO_{4\pm\delta}$ ($x = 0$, 0.05) were studied for the first time with the goal to evaluate their applicability as cathode materials for solid-oxide fuel cells. According to dilatometry data, the thermal expansion coefficients (TECs) of the oxides in air in the temperature range of 303–1123 K were 12.2 ($x = 0$) and 12.7 ppm K^{-1} ($x = 0.05$). A study of high-temperature crystal structure of $La_{1.2}Tb_{0.8}CuO_{4\pm\delta}$ revealed anisotropy of TEC along crystallographic axes (TEC(c)/TEC(a) = 1.35). Analysis of high-temperature electrical conductivity of the cuprates at various oxygen partial pressures showed that holes are the main charge carriers. The conductivity at 973 K in air was 0.3–0.6 S/cm. A possible reason for relatively low conductivity is the formation of Tb^{4+} cations at high temperature, which act as traps for main charge carriers. The results of this study indicate that $La_{1.2-x}Sr_xTb_{0.8}CuO_{4\pm\delta}$ may have only limited applicability as the cathode material in SOFC, for example, as thin film functional coatings.

Keywords: cuprates, dilatometry, high-temperature X-ray diffraction, high-temperature electrical conductivity

DOI: 10.1134/S0036023622060109

INTRODUCTION

Complex 3*d*-metal oxides with perovskite-like structure attract considerable attention in view of their possible practical use as electrode materials for various high-temperature electrochemical devices such as solid oxide fuel cells (SOFCs) [1–5]. Among the oxides that meet the requirements to cathode materials for intermediate-temperature SOFCs operating in the 500–800°C range, the of most interest are perovskites containing late 3*d* metals (Fe, Co, Ni, and Cu). This is due to their high oxygen-ion conductivity, which increases the cathode productivity in the intermediate temperature range [3].

Recently, the layered cuprates Ln_2CuO_4 with the perovskite-like structure have been studied as cathode materials for intermediate-temperature SOFCs [6–16]. Among the studied compounds, of considerable interest is Pr_2CuO_4, which has a simple chemical composition and combines low thermal expansion coefficient (TEC) (11.8 ppm K^{-1}) with high total electrical conductivity (~100 S/cm at 1173 K) [6]. This oxide, however, has a relatively low oxygen-ion conductivity, which is due to the presence of compressed Pr_2O_2 fluorite block in its crystal structure (T'-phase) [6]. Meanwhile, La_2CuO_4 with the K_2NiF_4 structure (T-phase), which contains a block with the rock salt structure, has a several orders of magnitude higher oxygen-ion conductivity, but has a low total conductivity (~15 S/cm at 1273 K), which virtually does not depend on temperature [17]. Among the cuprates $(A,A')_2CuO_{4-\delta}$, containing two A cations of different size, there are phases (T*-phases) that contain simultaneously rock salt and fluorite blocks in the crystal structure (Fig. 1). Such compounds are known, in particular, among the cuprates $Pr_{2-x}Sr_xCuO_{4-\delta}$ (x = 0.3, 0.4) [18]. A study of the high-temperature properties of these oxides demonstrated that they have acceptable electrical conductivity in air (~34 S/cm at 993 K for $Pr_{1.6}Sr_{0.4}CuO_{4-\delta}$) and higher oxygen-ion conductivity than Pr_2CuO_4; this is attributable to the presence of rock salt block in their structure [19]. It deserves mention that the presence of Sr^{2+} ions can be a drawback of these phases as cathode materials for intermediate-temperature SOFCs. These cations may induce increased reactivity on contact with the SOFC electrolyte based on the acidic oxide $Zr_{0.84}Y_{0.16}O_{1.92}$ (8YSZ). Among cuprates, there are also oxides that crystallize as the T*-phases and contain only rare earth metals as A cations. These phases include $La_{2-x}Tb_xCuO_4$ (x = 0.6–0.8) and $La_{2-x}Dy_xCuO_4$ (x = 0.8–0.9) [20].

The purpose of this study is to synthesize cuprates $La_{1.2-x}Sr_xTb_{0.8}CuO_{4\pm\delta}$ ($x = 0$ and 0.05) as T* phases and to study their high-temperature physicochemical

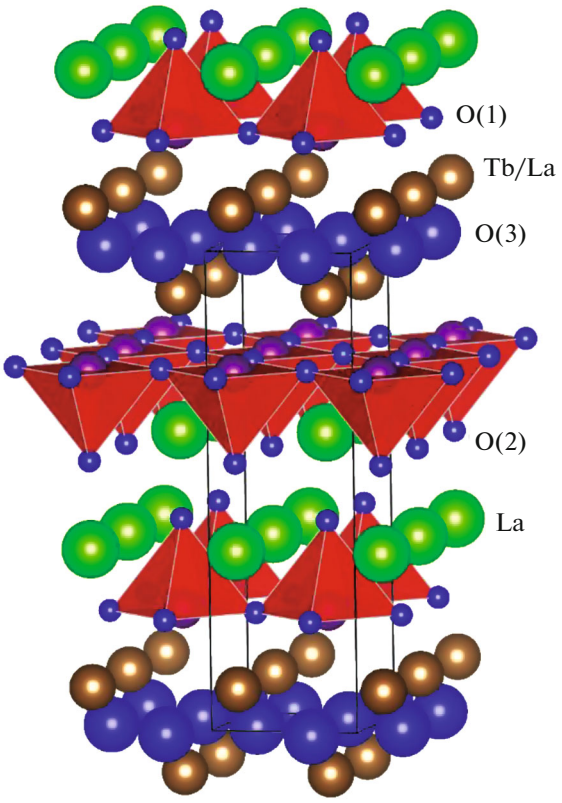

Fig. 1. Crystal structure of the T*-phase. The designations of atoms are given for $La_{1.2}Tb_{0.8}CuO_{4\pm\delta}$. The red polyhedra are the CuO_5 tetragonal pyramid. Oxygen atoms are marked in blue, La atoms are in green, and Tb/La are in brown.

properties, in particular, thermal expansion and electrical conductivity.

EXPERIMENTAL

The samples of $La_{1.2-x}Sr_xTb_{0.8}CuO_{4\pm\delta}$ ($x = 0$ and 0.05) were synthesized by the citrate method according to a reported procedure [20]. For this purpose, an aqueous solution obtained by dissolving stoichiometric amounts of La_2O_3 (99.999%), CuO (99.999%), and Tb_4O_7 in hot concentrated nitric acid and $Sr(NO_3)_2$ were added to a citric acid monohydrate melt $C_6H_8O_7 \cdot H_2O$ (50-fold molar excess). Prior to use, lanthanum oxide was annealed in air at 1173 K for 12 h in order to decompose carbonates formed upon long-term storage in air. The resulting mixture was evaporated in a porcelain dish on a gas burner until a thick caramel-like mass formed. The precursors obtained in this way were calcined at 923 K for 12 h. Then the powders were triturated in acetone in an agate mortar, pressed into pellets, and calcined in a tubular furnace in an oxygen flow at 1273 K for 48 h; the heating rate was 1 K/min. Then the pellets were triturated and pressed once again and calcined for 3–4 more times.

Powder X-ray diffraction study of polycrystalline samples was carried out at room temperature using a Huber G670 Guinier camera ($CuK_{\alpha1}$ radiation, λ = 1.5406 Å, Image Plate detector) and a Bruker D8-Advance diffractometer (CuK_α radiation, λ = 1.5418 Å). The results were analyzed resorting to the ICDD PDF-2 database. The unit cell parameters were refined using the STOE WinXPOW program package.

High-temperature X-ray diffraction was used to study the temperature dependence of the unit cell parameters of $La_{1.2}Tb_{0.8}CuO_{4\pm\delta}$ in the temperature range of 298–1073 K. The X-ray diffraction patterns were measured on a Bruker D8-Advance diffractometer equipped with a high-temperature XRK Anton Paar chamber (Germany). The crystal structures of the obtained compounds were refined using the TOPAS program package.

Thermomechanical measurements and determination of thermal expansion coefficients were performed using a NETZSCH DIL 402C dilatometer. The instrument was calibrated using a reference standard (reference material representing a 4.72 mm sapphire rod). The samples were formed as pellets with plane parallel faces. The pellet diameter was ≤6 mm and the pellet height was 4.5 to 5.5 mm. The measurements were carried out in a static air atmosphere in the temperature range of 303–1123 K at a heating rate of 5 K/min and under a 20 cN load. The results were treated using the Proteus Analysis software.

Thermogravimetric experiments were carried out using a Netzsch STA 449C thermal analyzer in an artificial air (20% O_2, 80% Ar) and in Ar/H_2 (8%) in the temperature range from 298 to 1073 K at a heating rate of 10 K/min.

The electrical conductivity of ceramic samples was measured by the four-probe method with direct current using a P-30S potentiostat (LLC Elins, Russia). The measurements were carried out at cyclic potential sweep from −100 to +100 mV at a rate of 20 mV/s in the temperature range from 373 to 1173 K in air, with the oxygen partial pressure being varied from 0.21 atm to 2×10^{-4} atm. The samples for measurements represented densely sintered cylindrical ceramics (8 mm in diameter and ~12 mm in height). The potential contacts were formed on the lateral surface of the sample with platinum paste. The electrical contacts were arranged by depositing the platinum paste on the end surfaces of the cylinder. After that, the sample was dried at 373 K for 1 h and then calcined at 1173 K for 5 h for complete removal of the organic components of the paste. The temperature was monitored using a Pt–Pt/Rh thermocouple located near the sample. The partial oxygen pressure was determined by a potentiometric oxygen sensor based on stabilized ZrO_2.

RESULTS AND DISCUSSION

The X-ray diffraction patterns of $La_{1.2-x}Sr_xTb_{0.8}CuO_{4\pm\delta}$ ($x = 0$ and 0.05) were indexed in the tetragonal system, space group $P4/nmm$, with the unit cell parameters $a = 3.862(3)$ Å, $c = 12.426(1)$ Å for $La_{1.2}Tb_{0.8}CuO_{4\pm\delta}$ and $a = 3.866(2)$ Å, $c = 12.466(3)$ Å for $La_{1.15}Sr_{0.05}Tb_{0.8}CuO_{4\pm\delta}$. It is known from the literature that the T*-phase can contain both oxygen vacancies and superstoichiometric oxygen located in tetrahedral interstices of the rock salt block [20]. In this study, the exact content of oxygen in the cuprates was not determined; however, since we reproduced the reported synthesis [15], the oxygen composition of the product can be assumed to be also nearly stoichiometric: $La_{1.2}Tb_{0.8}CuO_{4.05(3)}$ and $La_{1.15}Sr_{0.05}Tb_{0.8}CuO_{4.01(4)}$.

High-Temperature Thermal Expansion

Figure 2 shows the temperature dependences of the relative elongation of $La_{1.2-x}Sr_xTb_{0.8}CuO_{4\pm\delta}$ samples ($x = 0$ and 0.05). Both compositions showed almost linear thermal expansion in the temperature range of interest. The obtained linear TECs were similar, amounting to 12.2 ppm K^{-1} for $La_{1.2}Tb_{0.8}CuO_{4\pm\delta}$ and 12.7 ppm K^{-1} for $La_{1.15}Sr_{0.05}Tb_{0.8}CuO_{4\pm\delta}$. They were comparable with TECs of standard SOFC electrolytes based on stabilized zirconium dioxide 8YSZ (10.8 ppm K^{-1} [21]) and doped cerium oxide $Ce_{0.8}Gd_{0.2}O_{1.9}$ (20GDC, 12.8 ppm K^{-1} [22]). It is noteworthy that the dilatometric curves did not show a sharp chemical expansion effect, which is manifested as an increase in TEC with temperature and is mainly related to the loss of a part of oxygen by the oxide. This type of behavior is inherent, for example, in the cuprates $Pr_{2-x}Sr_xCuO_{4-\delta}$ ($x = 0.3$, 0.4) with T*-structure [21]. The absence of a sharp chemical expansion effect in the case of cuprates $La_{1.2-x}Sr_xTb_{0.8}CuO_{4\pm\delta}$ ($x = 0$, 0.05) is, most likely, due to the fact that the oxidation state of Cu cations in them is close to +2, which considerably hampers the loss of oxygen with temperature rise.

The crystal structure of $La_{1.2}Tb_{0.8}CuO_{4\pm\delta}$ at various temperatures was refined by the Rietveld method using the high-temperature powder X-ray diffraction data obtained in air in the temperature range of 298–1173 K. As the initial atomic coordinates, reported data were used [20]. Figure 3 shows the temperature dependences of the unit cells a and c of $La_{1.2}Tb_{0.8}CuO_{4\pm\delta}$. The calculated TEC values along the a and c crystallographic directions were 11.7 and 15.8 ppm K^{-1}, respectively. Thus, the phase demonstrated the TEC anisotropy with the coefficient TEC(c)/TEC(a) = 1.35. The linear TEC calculated from the temperature dependence of the unit cell volume as $V^{1/3}$ was 13.0 ppm K^{-1}, which is similar to the TEC value derived from the results of dilatometry (12.2 ppm K^{-1}).

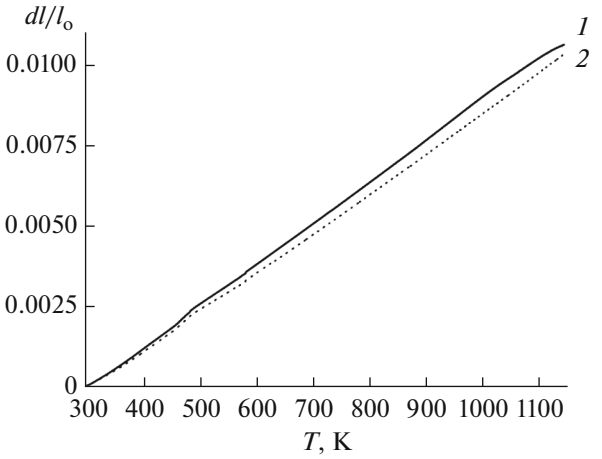

Fig. 2. Temperature dependences of the relative expansion of (*1*) $La_{1.15}Sr_{0.05}Tb_{0.8}CuO_{4\pm\delta}$ and (*2*) $La_{1.2}Tb_{0.8}CuO_{4\pm\delta}$ in air.

Apart from the calculation of TEC values, the temperature dependences of the key interatomic distances in $La_{1.2}Tb_{0.8}CuO_{4\pm\delta}$ were also analyzed (Fig. 4). In view of high errors in determination of oxygen atom positions from X-ray diffraction data, it is reasonable to discuss only the trends in the variation of distances between the cations and oxygen ions in the crystal structure of $La_{1.2}Tb_{0.8}CuO_{4\pm\delta}$. The most pronounced expansion with temperature increase was observed for the Cu–O(2) bond (55(2) ppm K^{-1}), which corresponds to the distance between the copper cation and the axial oxygen atom in the CuO_5 pyramid and for the Tb–O(1) bond (40(2) ppm K^{-1}) corresponding to the distance between the Tb cation of the fluorite block and the O1 oxygen atom of the CuO_2 layer located above the cation (Fig. 1). It is of interest that owing to the very fast increase in the Cu–O(2) bond length, the bond length between the La cation, which belongs to the rock salt block, and the same O2 atom, conversely, rapidly decreases with temperature increase (TEC(La–O(2)) = –29.4 ppm K^{-1}). This type of behavior is often characteristic of other T-phase oxides, e.g., $Pr_{1.25}Sr_{0.75}Cu_{0.25}Co_{0.75}O_{4-\delta}$ [23]. Mention should also be made of the fast increase in the Tb–O(1) bond length (Fig. 4c) with temperature. It is known from the literature that T'-phase cuprates have short R–O bonds within the R_2O_2 fluorite block, resulting in slight elongation of these bonds as the temperature increases. Meanwhile, long bonds between the cation R and oxygen atoms of the CuO_2 layer show more pronounced elongation with temperature. For example, in Sm_2CuO_4, these bonds are ~50% longer than bonds within the fluorite block [6]. In the case of cuprate $La_{1.2}Tb_{0.8}CuO_{4\pm\delta}$, these bonds differ by a factor of 3.7 (Figs. 4c and 4d). A probable reason is the variable oxidation state of Tb cations, which may affect the chemical nature of the Tb–O bond.

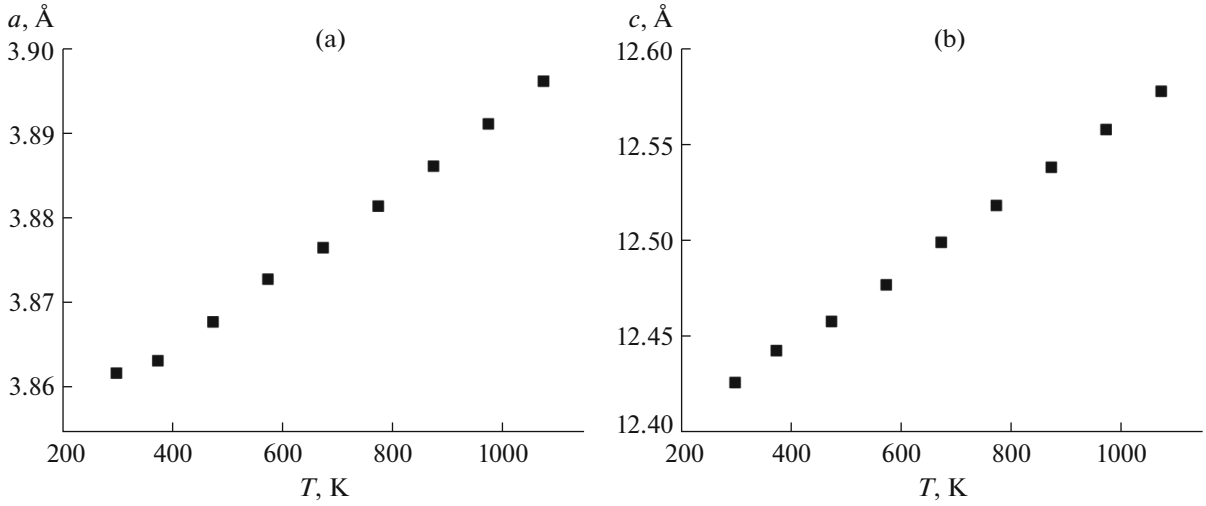

Fig. 3. Temperature dependence of the unit cell parameters (a) a and (b) c of $La_{1.2}Tb_{0.8}CuO_{4\pm\delta}$.

High-Temperature Electrical Conductivity

The temperature dependences of the electrical conductivity for $La_{1.2-x}Sr_xTb_{0.8}CuO_{4\pm\delta}$ ($x = 0$, 0.05) in air are depicted in Fig. 5. They obey the modified Arrhenius equation for the thermally activated behavior taking account of the fact that charge carriers in these compounds are small radius polarons:

$$\sigma T = A\exp\left(-\frac{E_a}{kT}\right), \quad (1)$$

where T is the absolute temperature; k is the Boltzmann constant; A is the pre-exponential factor; and E_a is the activation energy.

The electrical conductivity of both compounds shows a semiconductor behavior over the whole temperature range used under a partial oxygen pressure. At ~673 K, the slope of conductivity plots decreases, which is accompanied by a decrease in the activation energy (E_a) from 0.46 to 0.35 eV and from 0.41 to 0.31 eV for $La_{1.2}Tb_{0.8}CuO_{4\pm\delta}$ and $La_{1.15}Sr_{0.05}Tb_{0.8}CuO_{4\pm\delta}$, respectively. A somewhat higher conductivity of the Sr-containing material (at 973 K, 0.28 S/cm for $La_{1.2}Tb_{0.8}CuO_{4\pm\delta}$ and 0.56 S/cm for $La_{1.15}Sr_{0.05}Tb_{0.8}CuO_{4\pm\delta}$) is apparently due to the heterovalent replacement of La^{3+} cations by Sr^{2+}, which leads to increasing concentration of hole charge carriers ($h^\bullet$) according to the following quasi-chemical equations:

$$2SrO + CuO \xrightarrow{La_2CuO_4} 2Sr'_{La} + Cu^x_{Cu} + 3O^x_O + V^{\bullet\bullet}_O, \quad (2)$$

$$V^{\bullet\bullet}_O + \frac{1}{2}O_2(g) \rightarrow O^x_O + 2h^\bullet, \quad (3)$$

where Sr'_{La} is a strontium atom in a regular lanthanum position, Cu^x_{Cu} is a copper atom in a regular position, O^x_O is an oxygen atom in a regular position, $V^{\bullet\bullet}_O$ is an oxygen vacancy.

In order to find out the nature of charge carriers in the cuprates $La_{1.2-x}Sr_xTb_{0.8}CuO_{4\pm\delta}$, we studied the temperature dependence of electrical conductivity at various partial pressures of oxygen (Fig. 6). It should be noted that the conductivity of samples slightly increased with increasing partial pressure of oxygen. This implies that the main charge carriers in these compounds are holes located on copper ions ($Cu^\bullet_{Cu}$):

$$2Cu^x_{Cu} + V^{\bullet\bullet}_O + \frac{1}{2}O_2(r) \rightarrow 2Cu^\bullet_{Cu} + O^x_O. \quad (4)$$

The presence of oxygen vacancies may be due to oxygen loss both with temperature rise and due to a decrease in the partial pressure of oxygen in the gas phase. In the case of Sr-containing material, the formation of oxygen vacancies is also due to the heterovalent replacement of lanthanum cations by strontium cations (equation (2)).

It is noteworthy that up to 973 K, the temperature dependences of conductivity of $La_{1.2}Tb_{0.8}CuO_{4\pm\delta}$ followed similar patterns upon the variation of the partial oxygen pressure. However, at higher temperature, the electrical conductivity almost did not depend on pO_2. For $La_{1.15}Sr_{0.05}Tb_{0.8}CuO_{4\pm\delta}$, the temperature dependences of the conductivity changed in parallel with changes in the partial oxygen pressure.

In order to analyze the variation of the electrical conductivity as a function of pO_2 in more detail and to establish the mechanism of interaction of gas-phase oxygen with the solid, we plotted the conductivity isotherms in log-log coordinates (Fig. 7). The logσ–

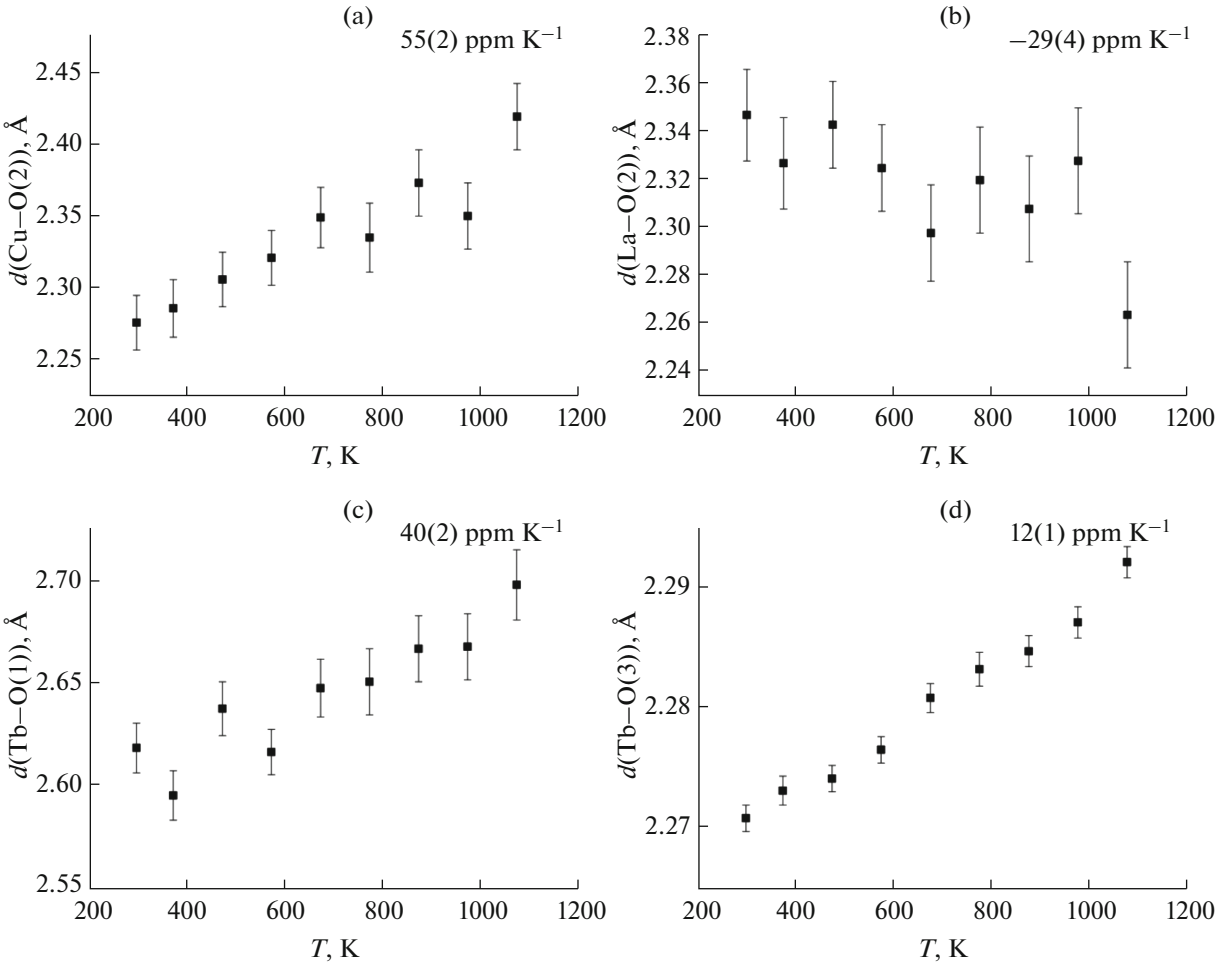

Fig. 4. Temperature dependences of the main interatomic distances in the crystal structure of $La_{1.2}Tb_{0.8}CuO_{4\pm\delta}$. The atom designations are the same as in Fig. 1.

$\log(p_{O_2})$ plots were linear. In the case of $La_{1.2}Tb_{0.8}CuO_{4\pm\delta}$ (Fig. 7a), the slope in the temperature range of 373–873 K was ~1/4. This behavior $\left(\sigma\infty p_{O_2}^{\frac{1}{4}}\right)$ may correspond to oxygen insertion into the vacant oxygen sites in the oxygen sublattice, according to equation (3) [24].

The temperature rise from 873 to ~1023 K leads to a decrease in the slope of the conductivity isotherms to ~1/6; as a result, oxygen insertion from the gas phase into the crystal lattice may be due to the formation of interstitial oxygen [25]:

$$\frac{1}{2}O_2(g) \Leftrightarrow O_i'' + 2h^\bullet. \quad (5)$$

Further temperature increase to 1173 K levels off the dependence of the conductivity on pO_2. A possible cause is partial transfer of Tb cations from +3 oxidation state (Tb_{Tb}^x) to +4 oxidation state ($Tb_{Tb}^\bullet$):

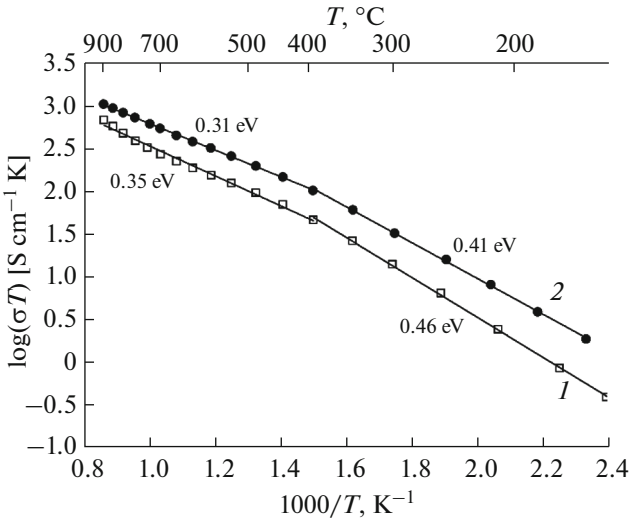

Fig. 5. Temperature dependences of the electrical conductivity of $La_{1.2-x}Sr_xTb_{0.8}CuO_{4\pm\delta}$ (x = (*1*) 0 and (*2*) 0.05) in air.

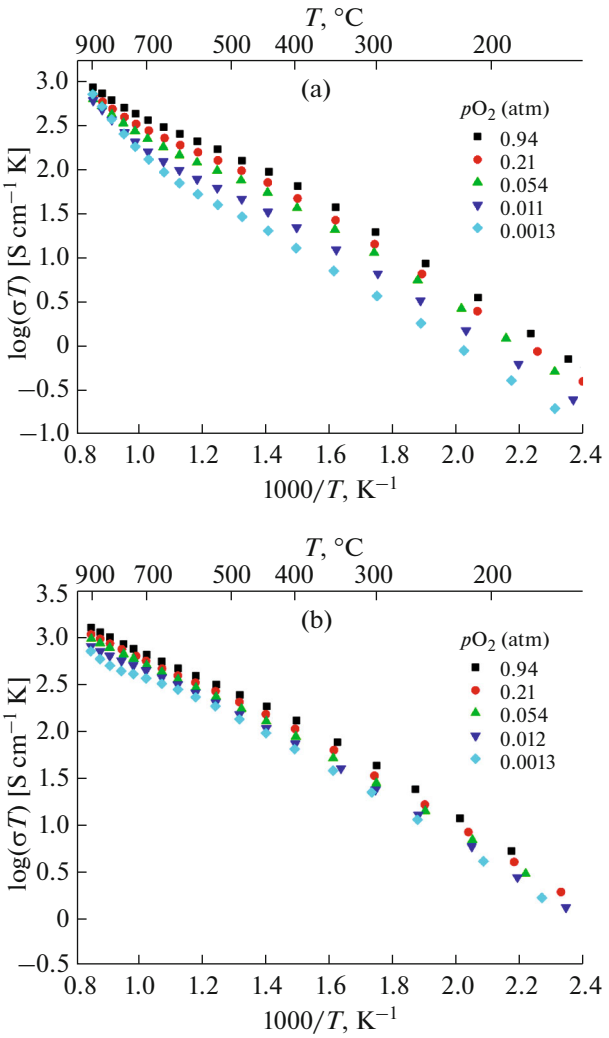

Fig. 6. Temperature dependences of the electrical conductivity of $La_{1.2-x}Sr_xTb_{0.8}CuO_{4\pm\delta}$, where x = (a) 0 and (b) 0.05, at various oxygen partial pressures.

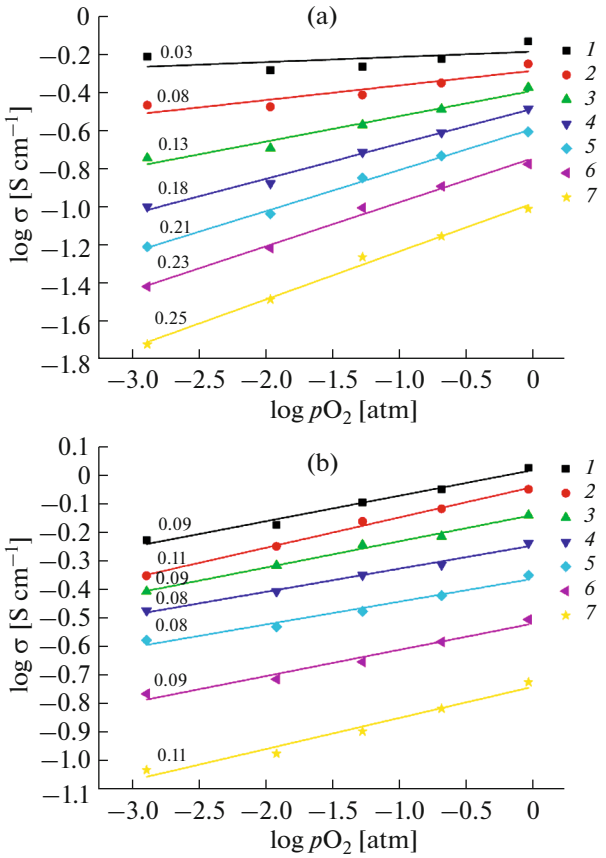

Fig. 7. Dependences of the electrical conductivity of $La_{1.2-x}Sr_xTb_{0.8}CuO_{4\pm\delta}$, where x = (a) 0 and (b) 0.05, on the partial oxygen pressure at various temperatures: (*1*) 1173, (*2*) 1093, (*3*) 1013, (*4*) 933, (*5*) 843, (*6*) 753, (*7*) 673 K (the numbers indicate the slope of the straight lines).

$$Tb_{Tb}^{x} \Leftrightarrow Tb_{Tb}^{\bullet} + e'. \quad (6)$$

As a result of thermal activation, the holes located on copper atoms can act as traps for the generated free electrons (e'):

$$Cu_{Cu}^{\bullet} + e' \Leftrightarrow Cu_{Cu}^{x}, \quad (7)$$

resulting in a decrease in the concentration of the main charge carriers; consequently, the conductivity no longer depends on the partial oxygen pressure under isothermal conditions.

The conductivity behavior of $La_{1.15}Sr_{0.05}Tb_{0.8}CuO_{4\pm\delta}$ as a function of pO_2 (Fig. 7b) differs from the behavior of $La_{1.2}Tb_{0.8}CuO_{4\pm\delta}$ described above. The slope of the conductivity isotherms versus pO_2 virtually does not change upon the variation of temperature. The slope is 0.10 ± 0.02, which apparently corresponds to predominance of oxygen insertion from the gas phase into the crystal lattice to give interstitial oxygen (equation (5), $\sigma \infty p_{O_2}^{\frac{1}{6}}$). Meanwhile, the presence of Sr^{2+} cations may induce association of oxygen vacancies, resulting in additional generation of interstitial oxygen [10]:

$$Sr_{La}' + O_O^x \Leftrightarrow \left(Sr_{La}' V_O^{\bullet\bullet}\right)^{\bullet} + O_i'', \quad (8)$$

which may somewhat decrease the concentration of hole charge carriers due to oxygen transfer to the gas phase:

$$O_i'' + 2Cu_{Cu}^{\bullet} \Leftrightarrow \frac{1}{2}O_2(g) + 2Cu_{Cu}^{x}. \quad (9)$$

Most likely, the possibility of these processes accounts for the clear-cut absence of a change in the slope of the conductivity isotherms versus pO_2 with temperature variation. This mechanism is supported by structural data reported in [20], which were obtained using low-temperature neutron diffraction. It follows from these data that partial replacement of Tb cations by Sr gives rise to oxygen vacancies in the

axial position of the CuO_5 pyramid (oxygen O(2), Fig. 1) and simultaneously increases the content of interstitial oxygen in the NaCl block.

CONCLUSIONS

Study of the high-temperature thermal expansion of layered cuprates $La_{1.2-x}Sr_xTb_{0.8}CuO_{4\pm\delta}$ ($x = 0$, 0.05) with T*-structure showed that they have linear TECs (12.2 and 12.7 ppm K^{-1} for $x = 0.0$ and 0.05, respectively) comparable with the TECs of standard SOFC electrolytes based on fluorite-like oxides 8YSZ and 20GDC. These TEC values are markedly lower than those for the cuprates $Pr_{2-x}Sr_xCuO_{4-\delta}$ with a similar crystal lattice (for example, for $x = 0.4$, TEC is 14.9 ppm K^{-1} at 423–773 K and 17.3 ppm K^{-1} at 773–1273 K [19]).

Study of high-temperature conductivity showed that the main charge carriers in these complex oxides are holes located on copper ions. The electrical conductivities of these compounds (0.3–0.6 S/cm at 973 K) are lower than those of the previously studied T*-phase oxides $Pr_{2-x}Sr_xCuO_{4-\delta}$ (34 S/cm at 993 K for $Pr_{1.6}Sr_{0.4}CuO_{4-\delta}$ [19]). A probable cause for the abnormally low electrical conductivity is the formation of Tb^{4+} cations, which act as traps for the main charge carriers, taking place at higher temperatures. Thus, due to low conductivity, the oxide phases $La_{1.2-x}Sr_xTb_{0.8}CuO_{4\pm\delta}$ ($x = 0$, 0.05) may find only a very limited use as cathode materials for intermediate-temperature SOFCs, e.g., as thin films.

FUNDING

The study was supported by the Interdisciplinary Scientific and Educational School of Moscow University "The Future of the Planet and Global Environmental Changes." The electrical conductivity measurements were carried out as a subject of the state assignment to the Institute of Problems of Chemical Physics, Russian Academy of Sciences (State Registration No. AAAA-A19-119061890019-5).

CONFLICT OF INTEREST

The authors declare that they have no conflicts of interest.

REFERENCES

1. A. Aguadero, L. Fawcett, S. Taub, et al., J. Mater. Sci. **47**, 3925 (2012). https://doi.org/10.1007/s10853-011-6213-1
2. A. J. Jacobson, Chem. Mater. **22**, 660 (2010). https://doi.org/10.1021/cm902640j
3. S. Ya. Istomin and E. V. Antipov, Russ. Chem. Rev. **82**, 686 (2013). https://doi.org/10.1070/RC2013v082n07ABEH004390
4. S. Ya. Istomin, N. V. Lyskov, G. N. Mazo, et al., Russ. Chem. Rev. **90**, 644 (2021). https://doi.org/10.1070/RCR4979
5. A. P. Tarutin, J. G. Lyagaeva, D. A. Medvedev, et al., J. Mater. Chem. A **9**, 154 (2021). https://doi.org/10.1039/D0TA08132A
6. M. S. Kaluzhskikh, S. M. Kazakov, G. N. Mazo, et al., J. Solid State Chem. **184**, 698 (2011). https://doi.org/10.1016/j.jssc.2011.01.035
7. N. V. Lyskov, M. S. Kaluzhskikh, L. S. Leonova, et al., Int. J. Hydrogen Energy **37**, 18357 (2012). https://doi.org/10.1016/j.ijhydene.2012.09.099
8. K. Zheng, A. Gorzkowska-Sobas, and K. Swierczek, Mater. Res. Bull. **47**, 4089 (2012). https://doi.org/10.1016/j.materresbull.2012.08.072
9. N. V. Lyskov, G. N. Mazo, L. S. Leonova, et al., Russ. J. Electrochem **49**, 747 (2013). https://doi.org/10.1134/S102319351308012
10. L. M. Kolchina, N. V. Lyskov, P. P. Pestrikov, et al., Mater. Chem. Phys. **165**, 91 (2015). https://doi.org/10.1016/j.matchemphys.2015.08.059
11. K. Mukherjee, Y. Hayamizu, C. S. Kim, et al., ACS Appl. Mater. Interfaces **8**, 34295 (2016). https://doi.org/10.1021/acsami.6b08977
12. A. P. Khandale, B. S. Pahune, S. S. Bhoga, et al., Int. J. Hydrogen Energy **44**, 15417 (2019). https://doi.org/10.1016/j.ijhydene.2019.04.055
13. L. dos Santos-Gómez, J. M. Porras-Vázquez, J. Hurtado, et al., J. Alloys Compd. **788**, 565 (2019). https://doi.org/10.1016/j.jallcom.2019.02.237
14. A. Niemczyk, A. Olszewska, Z. Du, et al., Int. J. Hydrogen Energy **43**, 15492 (2018). https://doi.org/10.1016/j.ijhydene.2018.06.119
15. V. N. Chaudhari, A. P. Khandale, and S. S. Bhoga, Ionics **23**, 2553 (2017). https://doi.org/10.1007/s11581-017-1999-8
16. H. Li and Zh. Cai, Q. Li, et al., J. Alloys Compd. **688**, 972 (2016). https://doi.org/10.1016/j.jallcom.2016.05.350
17. E. Boehm, J.-M. Bassat, M. C. Steil, et al., Solid State Sci. **5**, 973 (2013). https://doi.org/10.1016/S1293-2558(03)00091-8
18. H. Y. Hwang, S.-W. Cheong, A. S. Cooper, et al., Physica C **192**, 362 (1992). https://doi.org/10.1016/0921-4534(92)90842-Z
19. G. N. Mazo, S. M. Kazakov, L. M. Kolchina, et al., Solid State Ionics **257**, 67 (2014). https://doi.org/10.1016/j.ssi.2014.01.039
20. A. Lappas and K. Prasides, J. Solid State Chem. **115**, 332 (1995). https://doi.org/10.1006/jssc.1995.1142
21. G. Stochniol, A. Gupta, A. Naoumidis, et al., *Proceedings of the 5th International Symposium on Solid Oxide Fuel Cells (SOFC-V)*, Ed. by U. Stimming, et al. (Electrochemical Society, Pennington, 1997).
22. F. Tietz, Ionics **5**, 129 (1999). https://doi.org/10.1007/BF02375916
23. G. N. Mazo, S. M. Kazakov, L. M. Kolchina, et al., J. Alloys Compd. **639**, 381 (2015). https://doi.org/10.1016/j.jallcom.2015.03.081
24. D. J. L. Hong and D. M. Smyth, J. Solid State Chem. **102**, 250 (1993). https://doi.org/10.1006/jssc.1993.1029
25. D. J. L. Hong and D. M. Smyth, J. Solid State Chem. **97**, 427 (1992). https://doi.org/10.1016/0022-4596(92)90052-W

Translated by Z. Svitanko